Engineering Geology 357 (2025) 108369

Contents lists available at ScienceDirect

Engineering Geology

journal homepage: www.elsevier.com/locate/enggeo

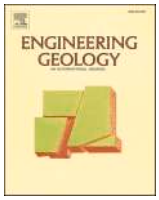

Advanced seismic microzonation of a medium size city over a deep sedimentary basin: The case of Foggia (Southern Italy)

N. Putrino [a], G. Cardillo [b], N. Carfagna [a], D. Albarello [a,c,*]

[a] Dipartimento di Scienze Fisiche, della Terra e dell'Ambiente, Università di Siena, Siena, Italy
[b] Practitioner Geologist, Foggia, Italy
[c] Consiglio Nazionale delle Ricerche, Istituto di Geologia Ambientale e Geoingegneria, Rome, Italy

ARTICLE INFO

Keywords:
Seismic microzonation
Seismic hazard
Seismic response analysis
Inversion
Geophysical data

ABSTRACT

Seismic microzonation is a basic element for emergency planning and developing effective risk reduction strategies. An application is presented of a cost-effective advanced strategy for the seismic microzonation of a large settlement: the city of Foggia in Southern Italy. Available geological and geophysical data have been reinterpreted and integrated with inversion techniques in order to reconstruct the seismostratigraphic structure of the local subsurface. Numerical simulations have been considered to infer the impact of these configurations on the local seismic hazard by taking into account uncertainty affecting the subsoil configuration. It has been demonstrated that the depth of the reference seismic bedrock plays a crucial role in hazard assessment, but its identification becomes challenging in the presence of a deep sedimentary basin, such as in the case of Foggia. Unlike most previous seismic microzonation studies in Italy, this work addresses uncertainties in expected seismic amplification effects and by considering alternative reference seismic bedrock configurations. On this basis, peak ground acceleration relative to 475y return period has been estimated for the study area by accounting for site effects and relevant uncertainty in the frame of a coherent probabilistic approach.

1. Introduction

Seismic hazard assessment is generally performed in two steps. First, seismic hazard is estimated at any reference soil condition on the basis of standard probabilistic approach (Cornell, 1968; McGuire, 1976) accounting for seismicity rates, distribution and geometry of seismic sources, and ground motion prediction equations determined at regional scale. Outcomes of this kind of analysis (e.g., Stucchi et al., 2011) are then implemented in the seismic code (e.g., CEN, 2005). As a second step, the possible impact of local seismostratigraphical and morphological configuration is evaluated to modify reference estimates and providing a more effective hazard estimate. In the seismic code, this last update is generally estimated at the scale of single manufact and to this purpose, specific experimental and numerical procedures are considered to provide this information (e.g. Kramer, 1996). However, when large scale hazard assessment is required to develop land planning policies aiming at seismic risk reduction or improving resilience at the scale of a municipality, budget limitations do not allow the general application of the standard procedures cited above. To face this problem, specific Seismic Microzonation (SM) strategies have been developed in Italy (SM Working Group, 2015; OPCM 3274, 2003) to support local administration in the definition of hazard maps at the scale of a Municipality. These procedures are designed to take into account available studies conducted for other purpose, along with cost-effective geophysical surveys and numerical simulations, within a coordinated strategy of collaboration between local professional subjects and academic institutions (Moscatelli et al., 2020). This approach focuses on identifying Seismically Homogeneous Microzones (SHMs), areas defined by similar expected responses to seismic ground motion amplification and earthquake-induces soil instability effects (such as liquefaction or landslides). Depending on available funds and data, three levels of detail constitute microzonation studies nowadays. At the first level, a reference seismo-geological model is defined based on the integration of existing data and cost-effective seismic surveys. At this level, SHMs are identified and described (qualitatively) in terms of expected co-seismic effects and only zones where 1D seismostratigraphical amplification effects are expected are identified. At the second level, for each of these SHMs, amplification effects are quantified often based on numerical approaches or supported by the application of seismic abacuses. The third level of the analysis focuses on the SHMs where complex effects are

* Corresponding author at: Dipartimento di Scienze Fisiche, della Terra e dell'Ambiente, Università di Siena, Siena, Italy.
E-mail address: dario.albarello@unisi.it (D. Albarello).

https://doi.org/10.1016/j.enggeo.2025.108369
Received 19 May 2025; Received in revised form 11 September 2025; Accepted 17 September 2025
Available online 18 September 2025

expected (e.g., liquefaction or 2D—3D seismostratigraphical amplification effects). In these zones, more advanced numerical modelling and specific site-specific investigations are carried out to achieve a more detailed definition.

Therefore, the outcome of seismic microzonation study is a patchwork of SHMs each characterized by a set of synthetic parameters quantifying expected phenomena. A limitation of this approach is that a number of artificial discontinuities are introduced at the contacts between contiguous SHMs, also the case that respective seismostratigraphical configurations varies smoothly. An attempt to attenuate this possible problem is presented below. Moreover, since microzonation outcomes are mainly devoted to support land planning activity operated by local Authorities, relative hazard estimates within the single municipality are of main concern, with no reference to absolute seismic hazard levels. To overcome this limitation, a more advanced approach is proposed here, where data collected by microzonation studies are re-examined and re-analysed to obtain a seismic hazard map (in terms of expected peak ground acceleration) of a municipality accounting for local effects and uncertainty inherently affecting large scale studies within a coherent approach considering the probabilistic character of the reference hazard map (Stucchi et al., 2011).

The proposed approach is applied to the city of Foggia (Southern Italy), a medium-sized town with approximately 150,000 inhabitants, situated in a flat and relatively deep sedimentary basin. A preliminary large scale seismic characterization of Northern Apulia area where Foggia is located has been provided by Paolucci et al. (2021). This study revealed that the seismic response of the Foggia area may be significantly affected by the presence of relatively deep seismic impedance contrasts (at depths of the order of hundreds of meters) which are not captured by seismic surveys performed for engineering purposes. Moreover, although the seismic hazard of Foggia can be considered moderate (PGA ≈ 0.15 g for a 10 % probability of exceedance in 50 years; http://esse1.mi.ingv.it/) compared to other Italian regions (in the range 0.05–0.35 g) the city has experienced severe earthquake damage in the past, most notably during the 1731 event (IX MCS; Locati et al., 2022). It worth noting that the above hazard estimate refers to reference soil conditions (rigid subsoil with shear wave velocities above 800 m/s) which is clearly unrealistic for the Foggia area where significant local amplification effects could be expected by the presence of soft sediments and seismic impedance contrasts at relatively high depths (hundreds of meters). The impact of this configuration cannot be captured by surveys commonly considered for anti-seismic design, which are limited to few tens of meters (NCT, 2018).

The following section provides a summary of the local geological setting, together with the data available for the seismic microzonation studies conducted in the area (Cardillo, 2021). Subsequently, the methodological approach adopted to reconstruct the seismostratigraphic configuration of the subsoil is described, including the data sources and the involved steps. Finally, outcomes of numerical simulations are reported as expected amplification and seismic hazard by considering the effect of relevant uncertainty within a coherent approach accounting for the inherent probabilistic character of seismic hazard estimates.

2. Geological setting and available geophysical information

A description of the geological setting of the study area can be found in Paolucci et al. (2021), which also includes outcomes of extensive geophysical surveys, borehole data and deep seismic reflection lines. In particular, the city of Foggia (Fig. 1) is located in the central portion of foredeep sedimentary basin, known as the *Bradanic Trough*, active from the Pliocene to the present day. The basin is located between an eastward verging complex tectonic assemblage of Mesozoic and Tertiary sedimentary units tectonically superimposed to each other, overthrusting a flexed carbonate platform (Apulian carbonates). By following Paolucci et al. (2021) the study area is located in the external foredeep depocenter where the depth of the Apulian carbonates is about 500 m. The oldest part of the infilling succession (Argille Subappennine formation during Middle Pliocene - Lower Pleistocene) consists of a turbiditic complex which lies on the Apulian carbonates. In particular, two distinct turbiditic cycles have been identified. The lower-one is composed of non-channelized basinal sequences (high-efficiency

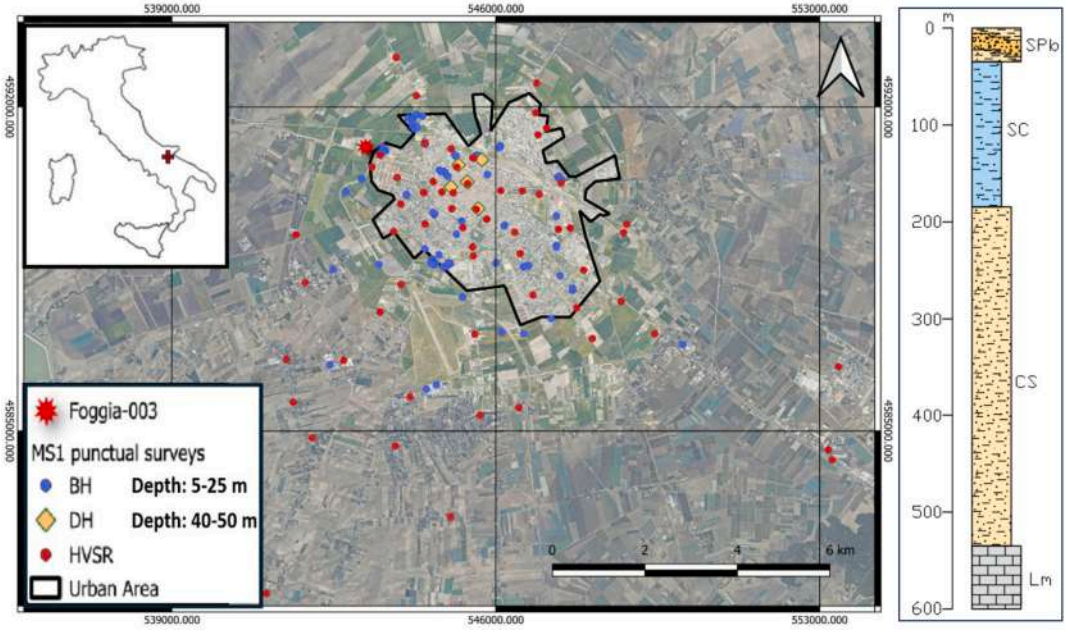

Fig. 1. Geographical overview of the study area and spatial distribution of the available subsurface data: Boreholes (BH), Down-Holes (DH), Horizontal to Vertical Spectral Ratio (H/V), deep explorative Borehole (Foggia-003). On the right, a representative lithostratigraphic column summarizes the typical vertical sequence observed in the area (Paolucci et al., 2021). From top to bottom: lenticular regressive deposits with heterogeneous grain size (SPb) and the two turbiditic cycles (upper and lower respectively indicated as SC and CS)—followed by the underlying carbonate bedrock (Lm). The column is based on the integration of deep exploratory boreholes and geotechnical logs within the urban area.

turbidites), while the upper-one is characterized by channeled turbiditic sequences (low-efficiency turbidites). A sandy horizon is interposed between the two depositional sequences and may represent a significant seismic impedance contrast (see Paolucci et al., for a discussion). The Quaternary outcropping portion overlying these deposits consists of a regressive succession of shallow-marine and/or continental-terraced deposits (Early–Late Pleistocene in age). These deposits, locally referred to as the "*Foggia Synthem*" consist of gravelly lenticular bodies interbedded with silty levels.

During preliminary seismic microzonation study (Cardillo, 2021), data from 84 geotechnical boreholes (from 5 up to 25 m deep), 93 single-station ambient vibration measurements using the H/V technique (Nakamura, 1989) and 5 downhole (DH) tests (Kramer, 1996) were collected. Additionally, results from 50 surface wave surveys using the MASW technique (Park et al., 1999) were available. However, MASW outcomes, limited to shallow depths and lacking associated uncertainty estimates, were not considered reliable constraints for reconstructing the subsoil configuration in this study.

In contrast, H/V data were regarded as particularly valuable due to their higher penetration depth and sensitivity to velocity contrasts. The H/V method relies on the measurement of spectral ratios of average spectral amplitudes of horizontal and vertical components of ambient vibrations and has been widely used for subsoil seismic characterization. It can be shown (e.g., Molnar et al., 2018) that the shape of these ratios as a function of the frequency reflects the subsoil seismic response and thus this technique plays a key role in advanced seismic microzonation studies, often in combination with other geophysical techniques (Vessia et al., 2021). In this work, H/V measurements represented the primary tool for inferring the deeper stratigraphic structure. After quality screening, 30 out of the 93 recordings were excluded due to poor signal quality, duplication, or excessive distance from the urban area. The spatial distribution of the data used in the following analyses is shown in Fig. 1.

3. Seismo-stratigraphic reconstruction from geophysical data

Lateral variation in the thickness of the shallowest regressive deposits can be determined using the available borehole data. These indicate the presence of superficial gravel bodies throughout the urban area, with thickness ranging based on the lenticular geometry of the deposits (Boggs Jr., 2006), but generally thicker in the central parts of the settlement. However, these data do not provide information on the seismic behaviour of these deposits, and they are limited to a depth of only a few tens of meters. To this purpose, available geophysical data (H/V analysis and DH surveys) have been considered, which represent a distributed source of indirect information about the subsoil seismo-stratigraphy (Fig. 1). The five downhole (DH) tests, which reach depths of about 40 m, fully penetrate the regressive deposits and extend to the top of the *Argille Subappennine* formation. As direct measurements of shear-wave velocities in the subsurface, the DH indicate significantly higher shear wave velocities in the gravelly layers (600–1100 m/s) compared to the silty facies of the regressive deposits and the underlying *Argille Subappennine* (400–500 m/s).

As regards the existing H/V curves, at first, they have been reprocessed to obtain a uniform dataset. To this purpose, raw data were reanalysed using "*Grilla*" software (Micromed Moho S.r.l.), employing 20-s window lengths with a 10 % triangular smoothing window. Noise disturbances were removed, and the overall quality of the signals was evaluated using the criteria proposed by Puglia et al. (2011). Seven measurements were excluded as they were considered unsuitable for further analysis.

H/V curves often exhibit two significant peaks in the low-frequency range (< 1 Hz), suggesting the potential presence of relatively deep seismic impedance contrasts. A first rough estimate of the possible depth of seismic impedance contrasts responsible for these maxima has been obtained in the quarter-wavelength approximation (Joyner et al., 1981), assuming an average Vs of ~600 m/s. This value reflects the increase of Vs with depth from ~400 m/s measured at 40 m (DH data) and is consistent with compaction trends observed in clay soils (Romagnoli et al., 2022) and with the higher velocities in the overlying gravel layers. The estimated depths are on the order of 500 m and 160–200 m, respectively. The deeper contrast is likely associated with buried Apulian foreland carbonates, while the shallower one is probably related to transition between the two turbiditic cycles identified by Paolucci et al. (2021).

Then, to improve robustness of this data set, H/V curves were grouped, under the assumption that similar curves correspond to comparable seismostratigraphic configurations. A hierarchical cluster analysis (Everitt et al., 2001) was performed by considering H/V curves in frequency range of 0.1–30 Hz and using the Pearson correlation index as the semblance parameter (e.g., Albarello et al., 2023). Five clusters were identified (Fig. 2), differentiated by the presence of the peaks and the corresponding frequencies, with a correlation index threshold of 0.5. In cases of ambiguity, a visual inspection of the curves has been used to manually assign them to appropriate clusters. Stratigraphic information from boreholes and DH data close to the single-station measurements were considered to constrain the inversion process and five representative H/V curves, one for each cluster (red curves in Fig. 2), were selected also accounting for their proximity to reliable stratigraphic data.

Almost all analysed measurements exhibit H/V curves with a clear minimum in the 1–10 Hz range. A similar pattern was observed by Di Giacomo et al. (2005) in the nearby city of Venosa, with similar stratigraphy to Foggia. The authors attributed this de-amplification to shallow velocity inversion caused by gravelly deposits.

Representative H/V curves have been used in inversion procedure with the Genetic Algorithm technique in order to infer the subsoil configuration in a 1D approximation (e.g., Fäh et al., 2001; Arai and Tokimatsu, 2004; Parolai et al., 2005; Picozzi et al., 2005; Foti et al., 2011). This last assumption implies that lateral variations are assumed to be relatively smooth: no evidence of faulting or sharp lateral discontinuity exists in the shallowest part of the sedimentary cover.

In the present application, the inversion procedure has been applied ten to twenty times at each site by retrieving the best fitting solution relative to each run. These best fitting solutions have been then considered, and the overall best fitting curve has been reputed as the general outcome. Details about the adopted procedure are reported in Picozzi and Albarello (2007). Two single-station measurements were located close to DHs, whose stratigraphic and seismic data were used to constrain the inversions. The remaining three measurements were inverted using stratigraphic data from nearby boreholes in the assumption that the same lithologies exhibit similar seismic behaviour across the studied area, with thickness variations only. Seismic analyses of the five DHs supported this assumption.

For deeper subsurface layers, where direct data were unavailable, loose constraints were applied to the depths of two anticipated lithological boundaries at 160–200 m and ~ 500 m. Depth variability was allowed between 100 and 300 m for the first boundary and 300–650 m for the second. Similarly, Vs was allowed a broad variability due to the lack of direct data. Despite this variability, the inversion results well aligned with stratigraphic data, indicating lithological boundaries at depths of ~150 m and ~ 400–500 m, and yielded Vs values consistent with available literature (Romagnoli et al., 2022).

Stratigraphic and velocity profiles obtained from the five representative inversions are shown in Fig. 3. For each cluster the obtained theoretical H/V curves form inversions are shown in comparison with experimental one, with details relative to the final misfit values for each inversion.

Notably, the number of layers in the regressive deposits varies due to their lenticular geometry. Considering all possible stratigraphic combinations for the five obtained models (Fig. 4), a generalized eight-layer model has been defined, consisting of, from top to bottom: Fill (F),

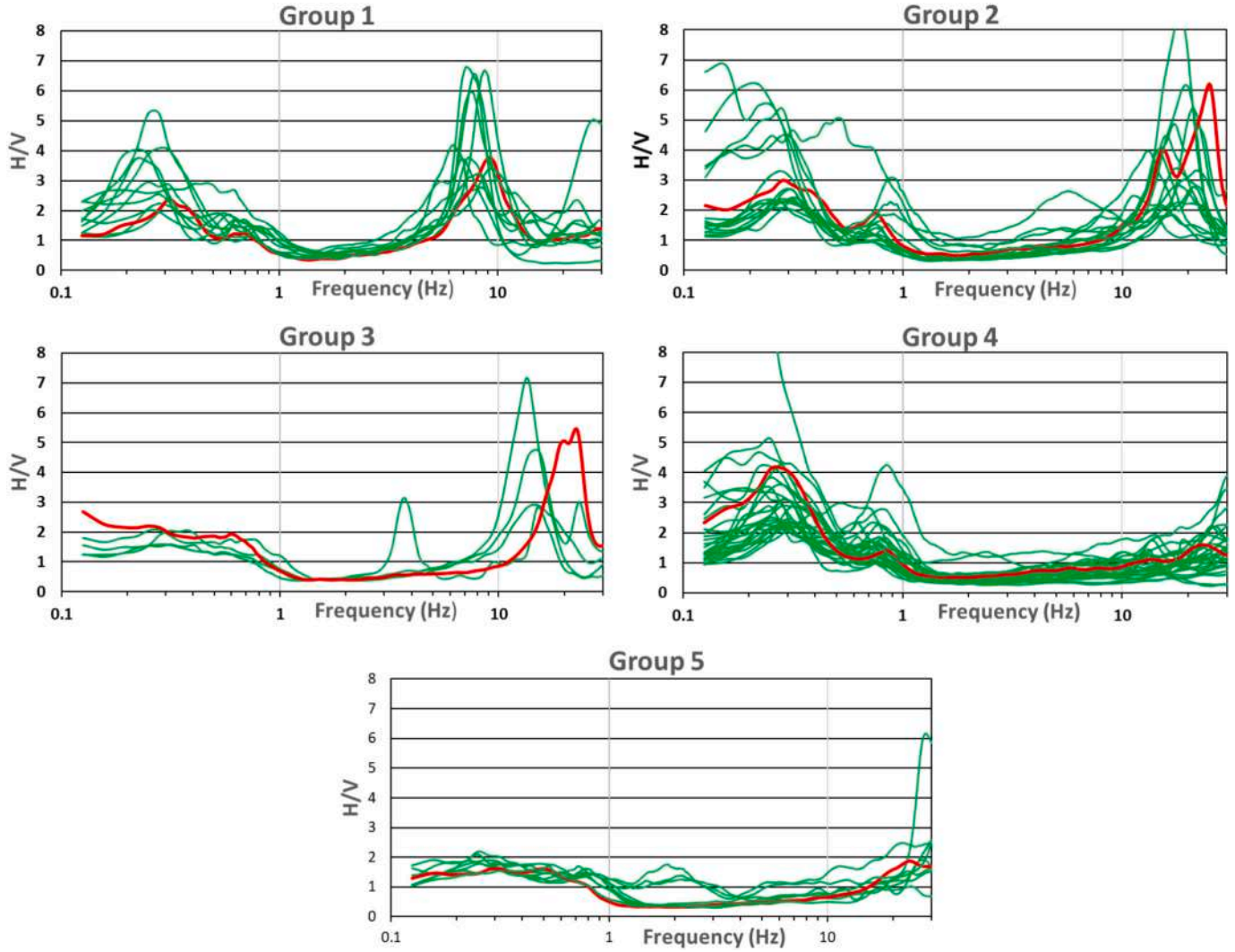

Fig. 2. Groups of H/V curves (in green) in each of the groups identified by the cluster analysis. The red curve is the one considered as representative for the respective group (see text for details). (For interpretation of the references to colour in this figure legend, the reader is referred to the web version of this article.)

Gravel (Gr-1), Sandy Silt (Ss), Gravel (Gr-2), Sand (S-1), Clay (C), Sand (S-2), and Limestone (Ls). The range of best fitting Vs values obtained for the relevant layer in the five inversions is also reported in Fig. 4. When the same lithology appears at different depths, numerical suffixes (1 and 2) distinguish respectively the upper from the lower unit.

The next step involved inverting remaining H/V curves using thickness, Vs, and Vp data derived from the models of the initial five representative inversions. Unlike these initial inversions, these subsequent ones are no longer constrained by direct stratigraphic data but by the results of the earlier inversions. In particular, models obtained from the inversion of a single representative curve are used as constraints for the entire cluster. For these inversions, upper and lower bounds were set around the values derived from the representative models, with a variability of ±5 % for layer thickness and Vs, and ± 10 % for Vp. These constraints are significantly more restrictive than those applied in the first inversions. Despite these tighter limits, the inversions successfully reproduced the H/V curves with a high degree of accuracy. This outcome reinforces the reliability of the representative models in guiding subsequent inversions and further supports the assumption of shared stratigraphic characteristics among curves within the same group.

4. 3D seismo-stratigraphic model

Results obtained from the constrained inversion of H/V curves have been used to build a 3D seismo-stratigraphic model of the study area as interpolation of the seismic layers represented in Fig. 4.

The ordinary kriging method (McBratney and Webster, 1986; Oliver and Webster, 1990) was used for the interpolation process. All the standard semi-variogram models (spherical, exponential, gaussian, linear, and circular) were considered to feed the kriging approach and provided the same outcomes with differences of the order of few centimeters, and thus negligible with respect to the objectives of this study. We ultimately adopted the spherical model, as it appeared appropriate for representing spatially continuous variables with finite correlation ranges, such as sedimentary deposits.

A total of seven surfaces corresponding to lithological boundaries were generated on an initial grid of 78 × 83 nodes with a resolution of 150 m, for a total of 6474 nodes. This configuration effectively captured the densely populated urban core while extending into adjacent rural areas. However, due to the limited availability of stratigraphic data in peripheral zones, maintaining the original grid resolution throughout the entire study area was unnecessary. To optimize subsequent analysis of the local seismic response, grid density was progressively reduced in areas farther from the urban centre, resulting in a refined grid of 1708 nodes while preserving essential spatial details. The seven surfaces were overlaid in order to obtain the thicknesses of the different lithologies at each grid point.

The regressive deposits posed a particular challenge due to their

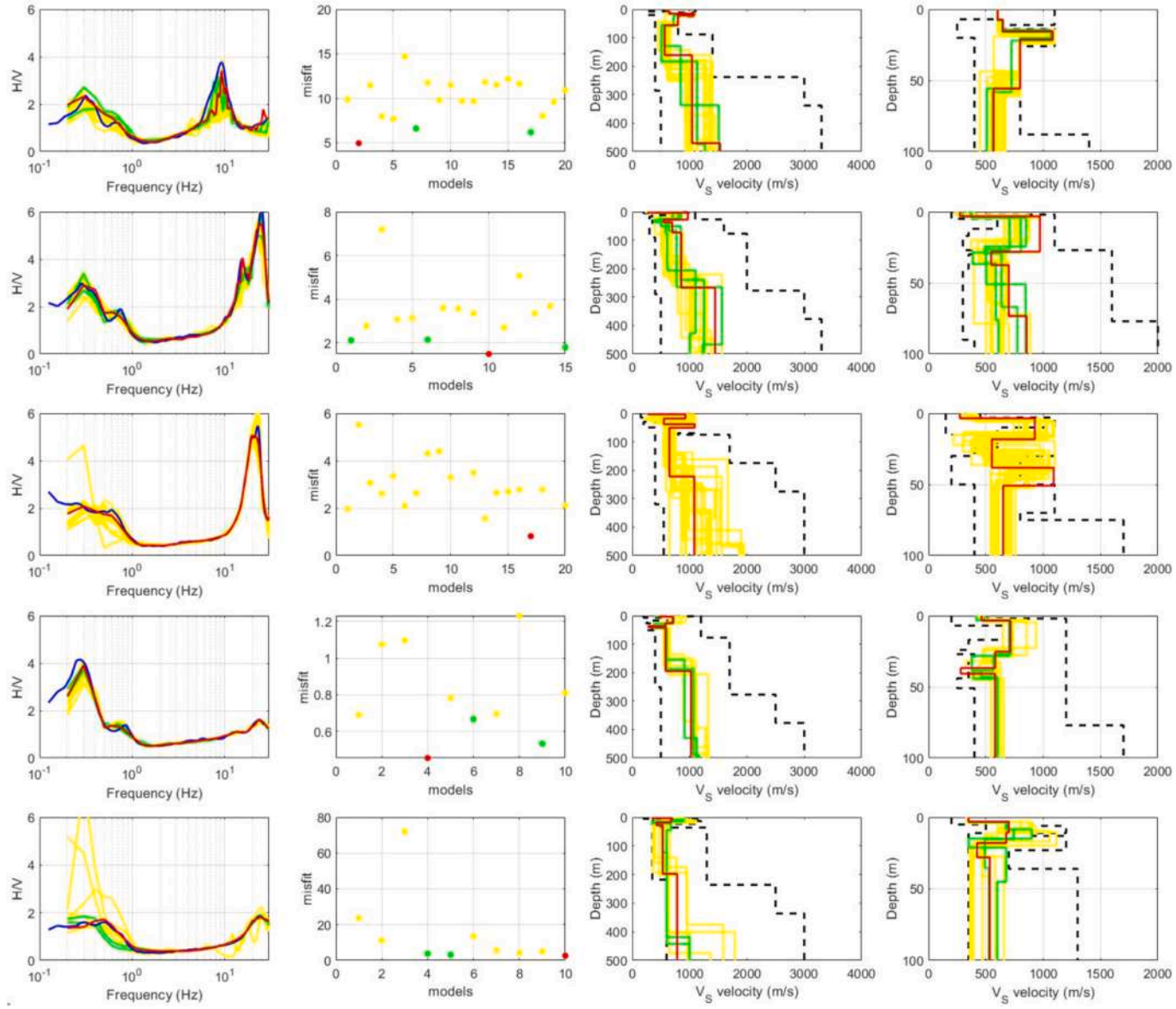

Fig. 3. Inversion of the 5H/V curves representative for each group identified by the cluster analysis. Plots on the same line refer to the inversion outcomes relative to each group. In the following columns are reported: the misfit values relative to the considered inversion runs, the corresponding Vs profiles down to a depth of 500 m and a focus on the shallower 100 m (the dashed lines indicate the range of Vs values considered in the inversion). The blue line indicates the experimental H/V curve, in yellow the outcomes relative to each inversion run, in red the values corresponding to the overall best fitting solution and in green alternative solutions characterized by a misfit value within 10 % of the one corresponding to the overall best fitting solution. (For interpretation of the references to colour in this figure legend, the reader is referred to the web version of this article.)

lateral variability and the reduction in data density with depth. While 152 stratigraphic profiles were available for the shallow layers, only 63 profiles (derived from H/V inversions) extended to the deeper strata. This data limitation occasionally led to inconsistencies in interpolation of layer thicknesses, with some nodes showing negative thickness values in the shallower strata. These negative values were generally lower, typically on the order of a few centimeters. Although their impact on the overall model was limited, such values were corrected to ensure stratigraphic continuity and coherence. A minimum thickness of 0.1 m was assigned to these layers, effectively representing erosional discontinuities (Boggs Jr., 2006) without compromising the structural integrity of the model. The obtained model, revealed to be fully compatible with available borehole data. In Fig. 5 the overall 3D model produced by the interpolation of the 1708 nodes is shown, with focus on two orthogonal cross-sections that well capture the lateral variability in terms of thickness of the considered layers.

5. Numerical simulation of the local seismic response

By following Italian Criteria for Seismic Microzonation (SM Working Group, 2015), outcomes of seismic microzonation studies are expressed in terms of seismic amplification factors (AF hereafter) computed at different period ranges of engineering interest defined as:

$$AF_{T_1-T_2} = \int_{T_1}^{T_2} \frac{SA_{out}(T)}{SA_{inp}(T)} dT$$

where SA_{out} and SA_{inp} respectively represent the ordinates of the response spectra at the surface and at the reference seismic bedrock. Areas with AF > 1 indicate stratigraphic amplification, whereas those with AF < 1 indicate expected de-amplification effect at the surface. Three ranges of periods are considered (AF1:0.1–0.5 s; AF2: 0.4–0.8 s; AF3: 0.7–1.1 s) respectively corresponding to common, high and

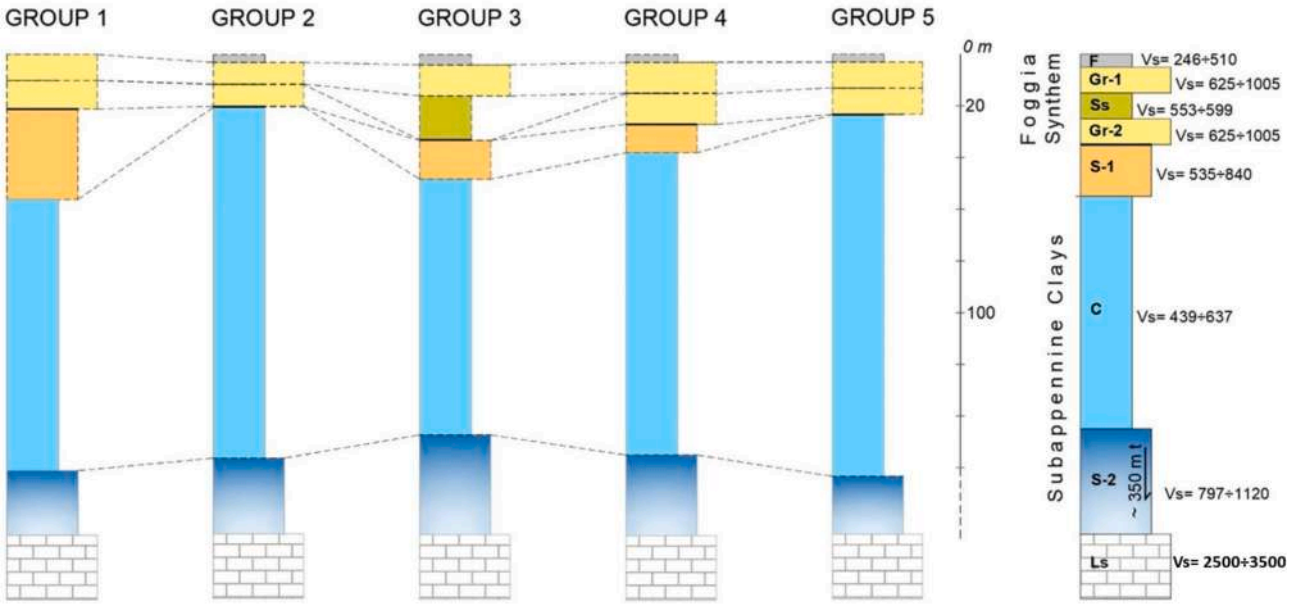

Fig. 4. Stratigraphic profiles obtained from the interpretation of the five representative H/V curves in Fig. 3 and a general stratigraphic model of the area with associated the range of best fitting Vs values (in m/s) relative to each layer and derived from the constrained inversion of H/V data (see text for details). The general stratigraphic model includes eight layers, though not all of them are consistently present across the study area, as shown in the five stratigraphic profiles: Fill (F), Gravel (Gr-1), Sandy Silt (Ss), Gravel (Gr-2), Sand (S-1), Clay (C), Sand (S-2), and Limestone (Ls). Vs values for the limestone unit are not derived from H/V inversion, as this method does not provide reliable estimates at such depths. Instead, indicative Vs values were assigned based on literature data, specifically from Rafavich et al. (1984).

seismically isolated buildings (Falcone et al., 2020, 2021; Lanzo et al., 2011; Lanzo and Pagliaroli, 2012; Mori et al., 2020; Pagliaroli et al., 2014; Santucci de Magistris et al., 2014). Along with this information, amplification factor relative to Peak Ground Acceleration (PGA) has been also considered.

Simulations have been performed in the frame of the Random Vibration theory (Kottke and Rathje, 2008) by assuming as a reference event earthquake with magnitude range 6.0–6.5. In this approach, input motion is supplied in terms of a response spectrum in acceleration (no time history is required). In the case here considered, the uniform hazard spectrum is the one supplied by National Hazard Map for the city of Foggia corresponding to an exceedance probability of 10 % in 50y (Stucchi et al., 2011) and relative to a reference subsoil configuration (flat outcrop of a rigid subsoil characterized by shear waves velocity above 800 m/s). The choice of this reference value is merely conventional and does not rely on any seismological or-geotechnical consideration. It depends on the availability of a number of accelerometric data at relatively rigid soil sufficient for the parameterization of ground motion prediction equations implemented in the standard procedure for above hazard assessment in Italy (and more generally in Europe): actually, the reference ground motion to be considered for anti-seismic design and site response assessment is assumed to be known (with relative uncertainty) at the reference engineering bedrock (Vs above 800 m/s) irrespective the actual subsoil configuration. AF values relative to the considered area have been obtained by numerical simulations considering linear-equivalent approach which is reputed adequately accounting for non-linear soil behaviour (PGA remains below 0.3 g), which is consistent with the Italian reference hazard for a 475-year return period at Foggia (Falcone et al., 2021). In the numerical simulations, no impedance correction was applied at the input boundary, consistent with standard practice in equivalent-linear 1D site response analysis.

To account for uncertainty affecting model parameters a number of stochastic simulations have been performed at each location (at each grid node) using the software NC92Soil (Acunzo et al., 2024). In each simulation, Vs values are randomly extracted by log-normal probability distribution with a depth dependent average and variance. Following Romagnoli et al. (2022) the shape of the relevant distribution and of the interlayer correlation depend on the prevalent lithology within each layer. The random values extracted in this way were constrained within the range of available experimental values (Fig. 3). In the lack of local information, literature data were considered for possible Vs values within the deep carbonate layer. To define realistic Vs boundaries for this layer, we referred to Rafavich et al. (1984), who measured Vs values for different carbonate deposits under simulated in-situ conditions, reporting a range between 2500 and 3500 m/s.

The same procedure has been adopted to randomly select shear modulus decay and damping curves within a variability range as a function of depth and dominant lithology by considering empirical relationships provided by Gaudiosi et al. (2023) and Pieruccini et al. (2024). Layer thickness relative to the Quaternary outcropping units have been kept as fixed since they are well constrained by borehole data. The same holds for the depth of the Carbonate units at the bottom of the Argille Subappennine formation which are well constrained by a deep borehole 'Foggia-003' close to Foggia (ISPRA (Istituto Superiore per la Protezione e la Ricerca Ambientale), 2025). The possible location of the transition between upper and lower turbiditic layers within the Argille Subappennine formation is instead weakly constrained and thus the respective depth has been randomly variated between 150 and 250 m.

For each of the 1708 grid nodes, 100 random profiles were generated, resulting in a total of 170,800 1D stochastic simulations. The relevant seismic and geotechnical profiles relative to each simulation have been randomly generated by considering the empirical lognormal distributions parameterized by following Romagnoli et al. (2022), Gaudiosi et al. (2023) and Pieruccini et al. (2024) and depending on the prevalent lithology and depth. As concerns Vs values, the relevant randomized values have been constrained within the ranges of variation determined by the constrained inversion of H/V data and reported in Fig. 4 (and in the supplementary material). This ensured a statistically robust dataset for amplification factor analysis and the respect of the constraints provided by local information.

One of the primary factors influencing the amplification factor (AF)

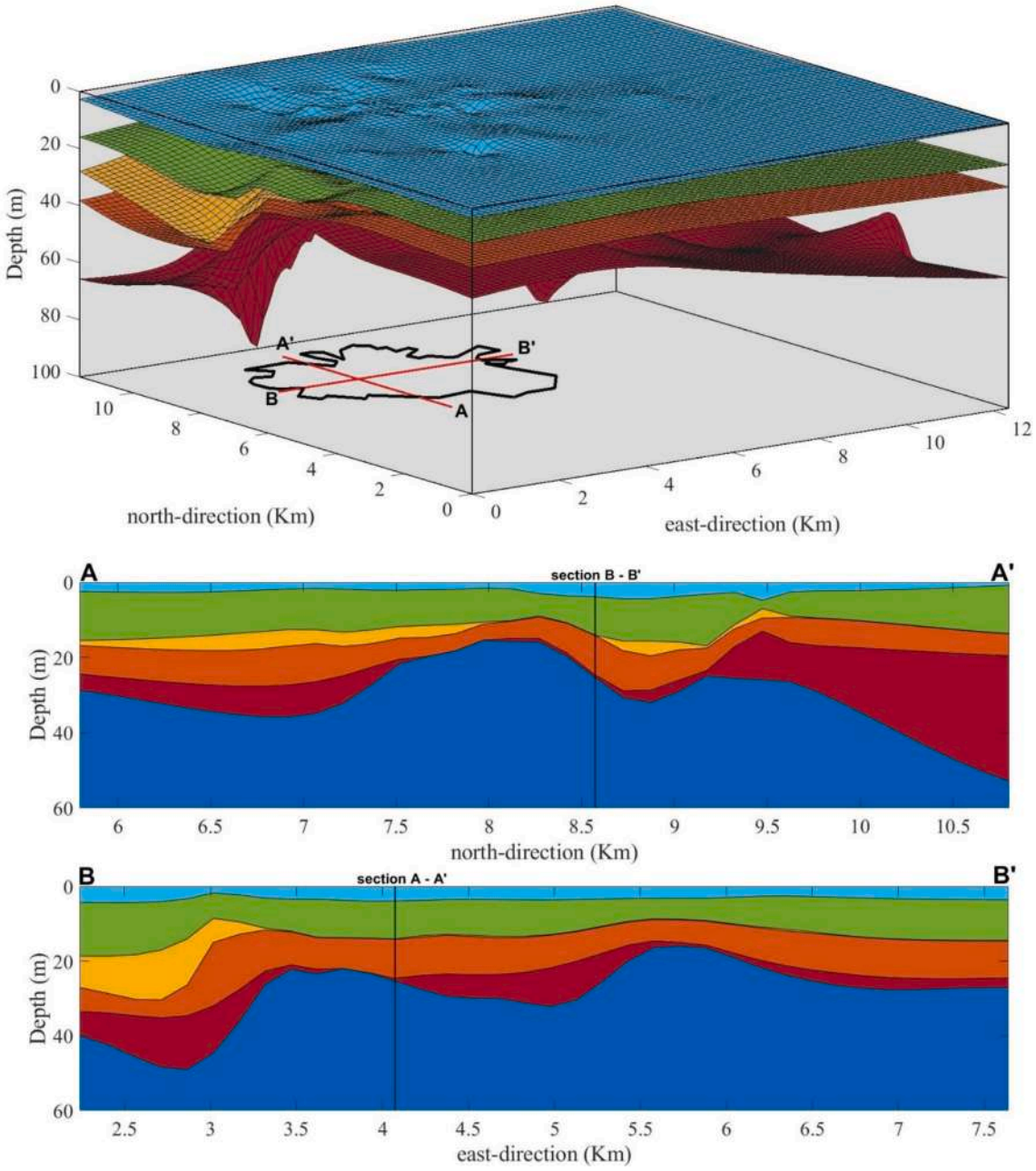

Fig. 5. The figure shows a 3D subsurface model of the upper 100 m. The top part provides a perspective view of the first five stratigraphic surfaces: F (light blue), Gr-1 (green), Ss (yellow), Gr-2 (orange), and S-1 (red). Deeper stratigraphic surfaces are not displayed for clarity and scale considerations. At the base of the model, the perimeter of the inhabited area is projected, with the traces of two cross-sections oriented North-South and East-West. These sections are shown in the lower part of the figure. The dark blue layer in the sections represents the uppermost part of the C strata. Both the 3D model and the cross-sections exhibit significant vertical exaggeration. For simplicity, the model is shown using relative coordinates, where the point (0,0) corresponds to the location X: 541642 m; Y: 4581490 m in the WGS 84 UTM 33 N reference system (EPSG 32633). (For interpretation of the references to colour in this figure legend, the reader is referred to the web version of this article.)

is the definition of the reference seismic bedrock where the input motion is applied in the numerical simulations (e.g., Pieruccini et al., 2024). As shown in Fig. 3, several lithologies in our stratigraphic model, including Gr-1, Gr-2, S-1, S-2, and Ls, exhibit Vs values that may reach the Vs threshold (800 m/s) according to Italian Seismic Code. It is important to note, however, that defining the reference seismic bedrock involves more than just identifying where Vs exceeds 800 m/s; the velocity must also remain stable with depth, without significant decreases, as emphasized in the NTC18 (2018) guidelines. Based on this criterion, the uppermost layers (*Gr-1*, *Gr-2*, and *S-1*) cannot be considered as a reference seismic bedrock due to the presence of underlying clay deposits, and the first layer that satisfies both conditions is *S-2*. However, the reference seismic bedrock may correspond to either S-2 or Ls horizons since in both cases expected Vs values exceed 800 m/s. It worth to note that, despite of the formal definition of a reference seismic bedrock, the strong impedance contrast between *S-2* and *Ls* may play a role in the seismic response assessment, as *Ls* is expected to have a significantly higher Vs than the overlying sandy deposits. To account for both possibilities, we performed numerical simulations twice: once with S-2 as the reference seismic bedrock and once with *Ls*. The impact of the different choices of the reference seismic bedrock on the expected amplification effects relative to a single location within the study area is

reported in Fig. 6.

One can see that selecting the *Ls* layer as the reference seismic bedrock leads to significantly higher amplification factors across all considered frequency ranges, compared to simulations based on the shallower *S-2* layer. The summary of outcomes of the 1D numerical simulations for the study area are presented in Fig. 7 by considering distribution of median AFs obtained by the two possible choices of the reference seismic bedrocks for each of the grid nodes.

These differences also result dependent on the location as shown in Figs. 7 and 8. In these figures the 84° percentile (mean + 1σ) of the distribution of AF values retrieved at each site has been considered as representative of the local amplification effect. This choice is in line with the one proposed by Andreotti et al. (2018) to implement the amplification factors relative to the 1D seismostratigraphic configuration in the seismic code by accounting for the relevant uncertainty within the probabilistic approach underlying the standard seismic hazard map.

On this regard, as shown in Fig. 8, simulations made using *S-2* as the reference seismic bedrock yield relatively homogeneous AF distributions over the urban area of Foggia: most of values remain within a moderate amplification range (AF $\leq$ 1.30), with only limited zones exhibiting slightly higher values for longer periods (e.g., in the ranges 0.1–0.5 s and 0.7–1.1 s). This pattern reflects the comparatively lower impedance contrast between surface deposits and the underlying *S-2* sandy layer, resulting in a less pronounced stratigraphic response.

On the contrary, simulations based on the deeper carbonate *Ls* layer produce a more complex and variable amplification scenario (Fig. 9). AF values are generally higher across all maps (in PGA and 0.7–1.1 s), with the most substantial amplifications observed for longer period intervals (notably AF3). In these maps, large portions of the study area exhibit AF values exceeding 1.75, with some areas even surpassing 2.0.

Moreover, the spatial distribution of the amplification in Fig. 9 suggests that the presence of thick, soft sediments plays a key role in focusing seismic energy, especially for low-frequency content. In contrast, the relatively flat response seen in Fig. 8 implies that using a shallower, intermediate-velocity layer as a reference seismic bedrock may lead to an underestimation of expected site effects in similar geological settings.

To provide a quantitative representation of the expected ground shaking in terms of pseudo-accelerations, the amplification factors were applied to the baseline seismic hazard values defined at the national scale for a 10 % probability of exceedance in 50 years. This integration was performed following the probabilistic formalization proposed by Albarello and Paolucci (2024). The results of this operation are presented in Fig. 10 and show the possible impact of computed AF values on the local seismic hazard.

As expected, the deep reference seismic bedrock configuration

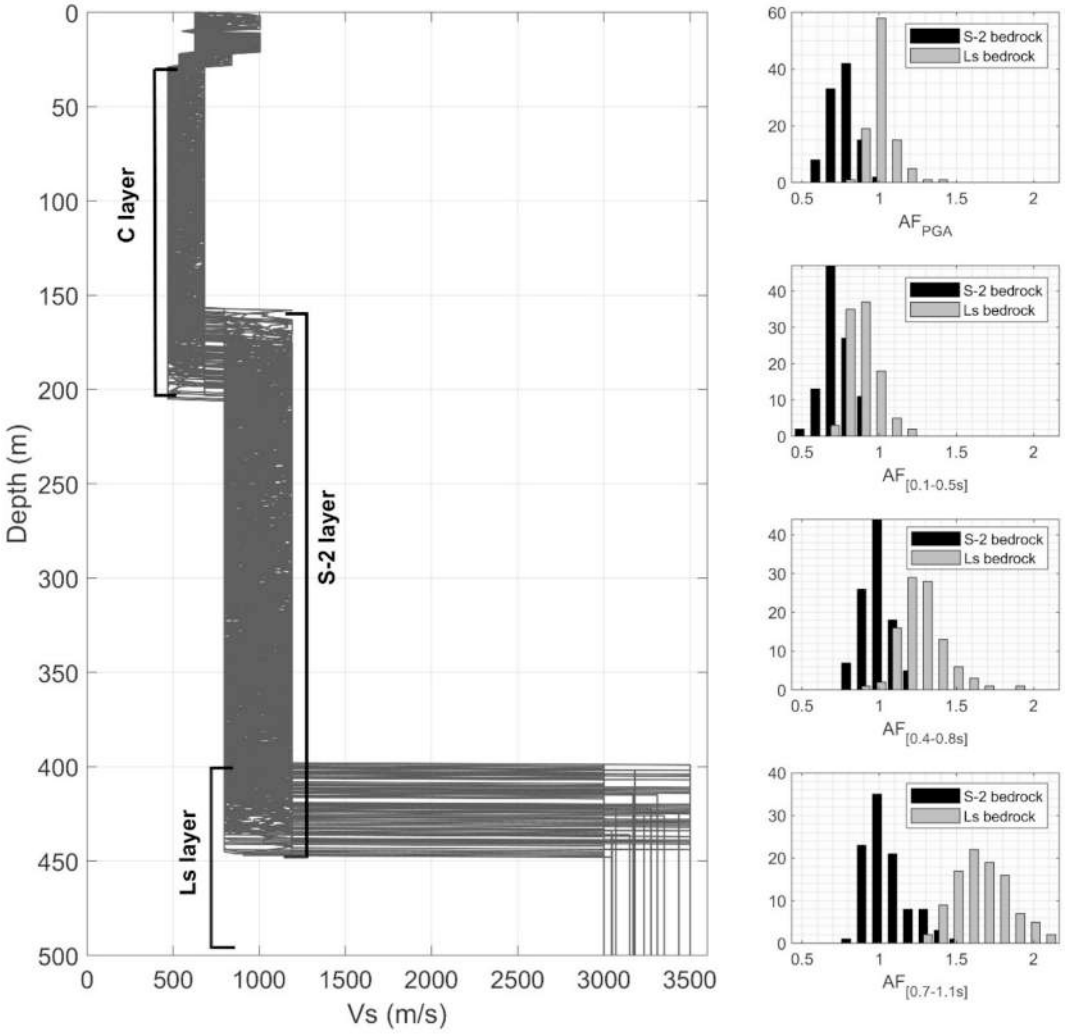

Fig. 6. Comparison between distribution of amplification factors in the different vibration periods obtained by assuming the two possible reference seismic bedrocks (S-2 and Ls respectively) at a site within the study area. On the right, the considered Vs profiles considered in numerical simulations by randomly varying the relevant parameters (Vs and thicknesses in the plot). On the right, the corresponding distributions of AF values.

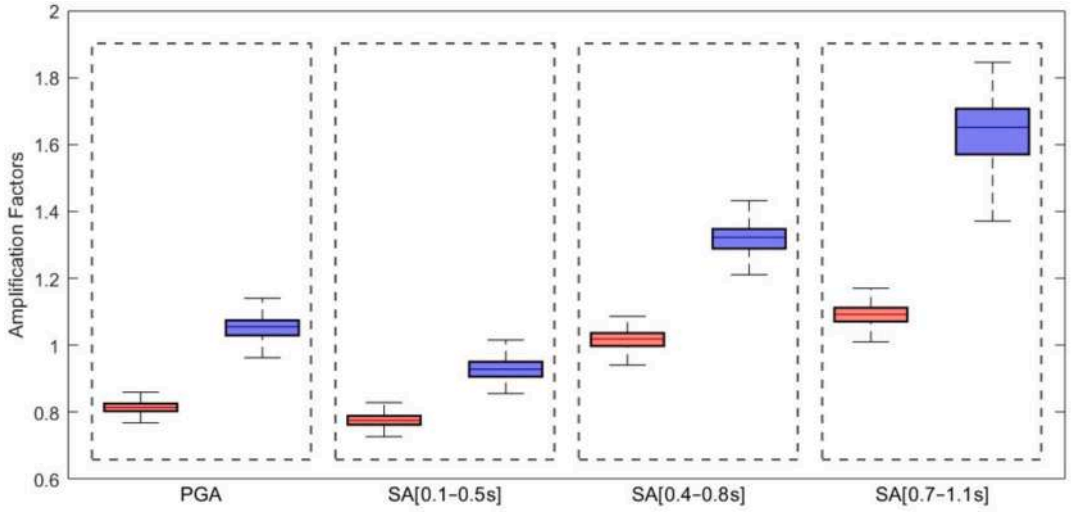

Fig. 7. Comparison between distribution of median amplification factors in the different vibration periods obtained by assuming the two possible reference seismic bedrocks: the shallower (S-2) in red and the deeper (Ls) in blue. For each interval of periods (dotted frame) the boxes include the central 50 % of the whole distribution of median values, the line inside the box indicates the overall median; the vertical whiskers include the values within 1.5 times the respective quartile. (For interpretation of the references to colour in this figure legend, the reader is referred to the web version of this article.)

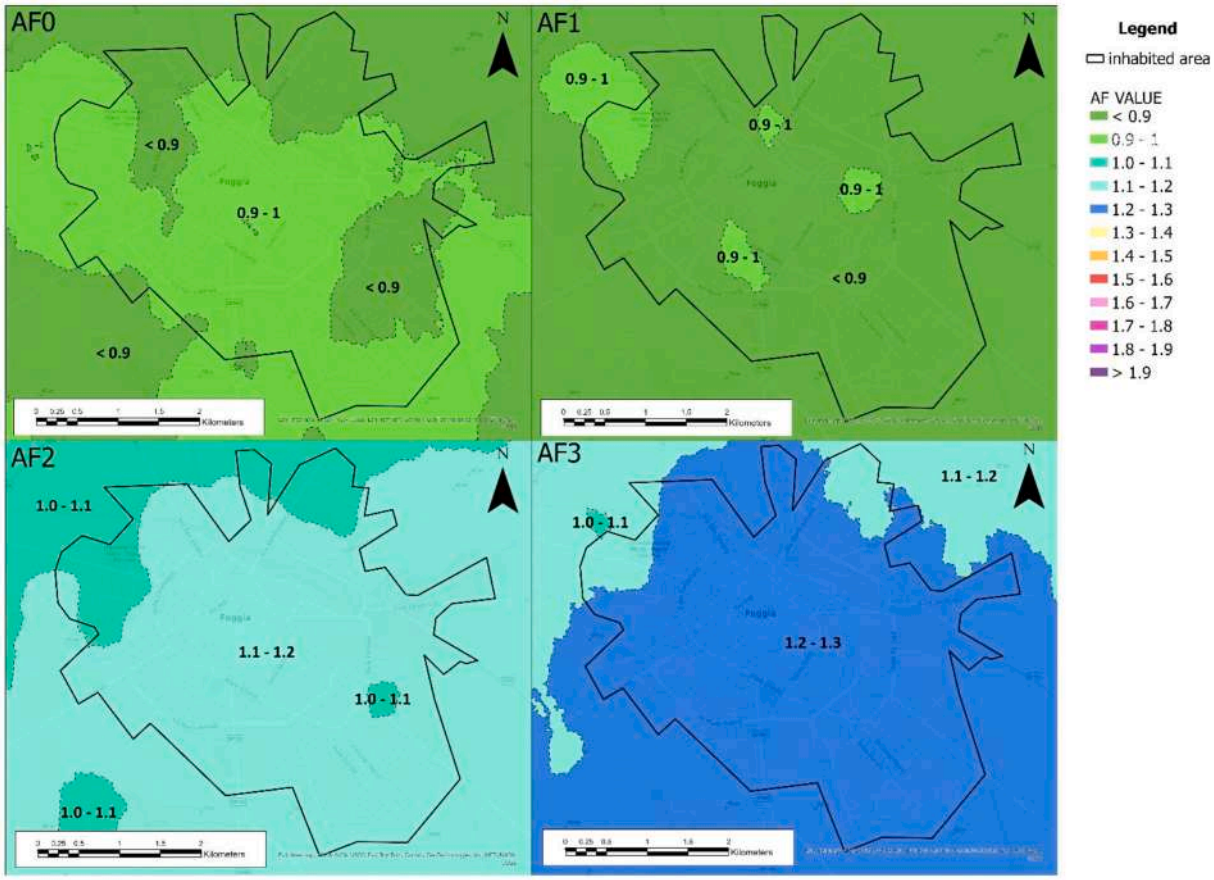

Fig. 8. Maps of amplification factors relative to PGA (AF0) and to the periods 0.1–0.5 s (AF1), 0.4–0.8 s (AF2) and 0.7–1.1 s (AF3). Values refer to simulations with the S-2 layer considered as the reference seismic bedrock. In order to adopt the approach proposed by Andreotti et al. (2018), the values correspond to 84° percentile of the distribution of the AF values obtained in the random simulations relative to each node. Numbers in the plots represent the range of amplification factors estimated for the relevant area. Values below 1 indicate and expected de-amplification with respect to the reference input motion.

results in systematically higher ground shaking levels across all periods, especially at 0.5 s and 1 s, where values exceed 0.35 g over wide sectors of the urban area.

New pseudo-acceleration values are direct consequence of the higher amplification factors associated with the thick, low-rigidity sedimentary cover above the Ls layer, as previously highlighted. The spatial

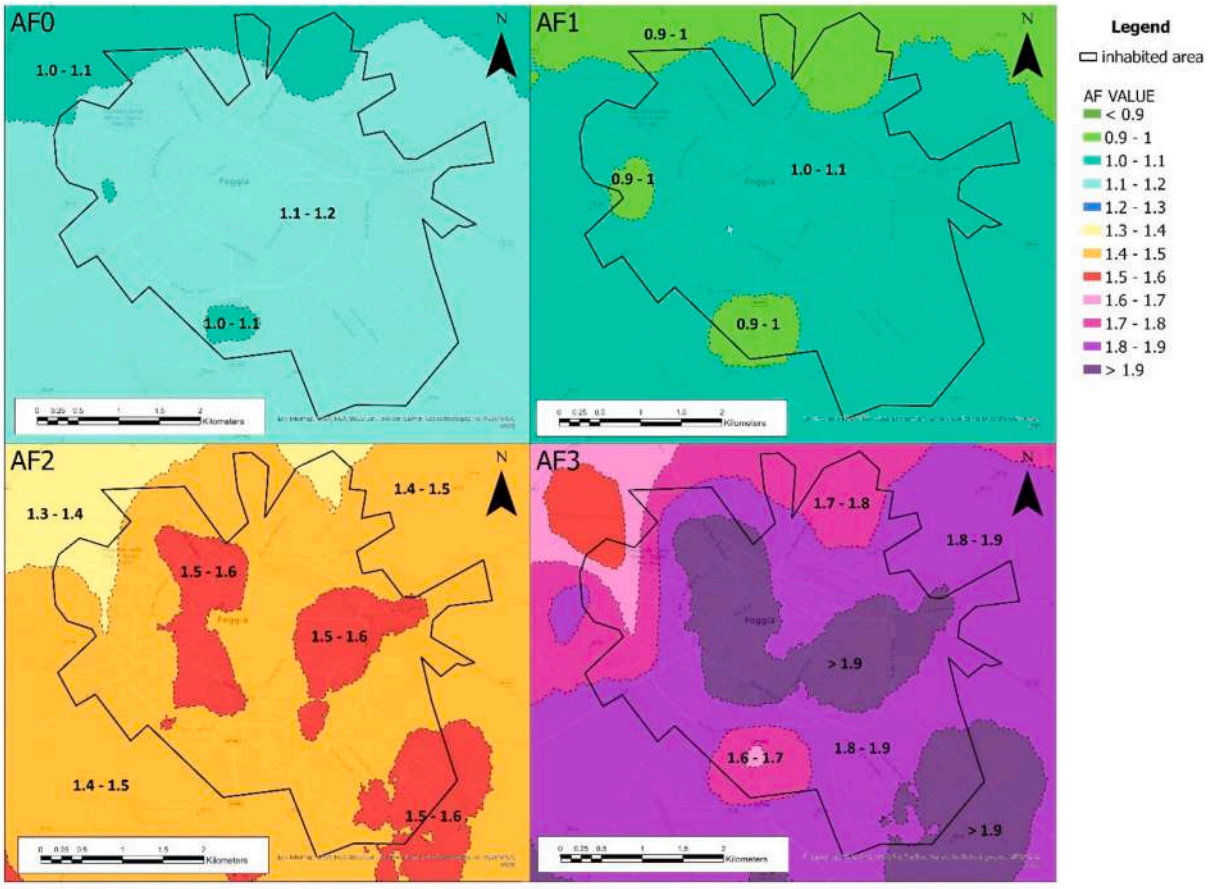

Fig. 9. Maps of amplification factors relative to PGA (AF0) and to the periods 0.1–0.5 s (AF1), 0.4–0.8 s (AF2) and 0.7–1.1 s (AF3). Values refer to simulations with the Ls layer considered as the reference seismic bedrock. See supplementary material for the values obtained at each node of the grid considered for numerical simulations. For details, see caption of Fig. 8.

variability in acceleration values further emphasizes the inhomogeneous seismic response of the area.

The comparison between different reference seismic bedrock definitions also stresses the need for site-specific criteria in selecting reference horizons, especially in areas characterized by complex stratigraphic settings and deep sedimentary basins such as the one investigated in this study. In this context, passive seismic methods have proven to be an essential investigative tool, offering excellent depth penetration and a strong cost-benefit ratio, making them particularly well-suited for extensive microzonation studies and seismic hazard assessments.

6. Conclusions

This study presents a comprehensive advanced approach to seismic microzonation for the city of Foggia using both geophysical and numerical methods. With respect to standard microzonation study, a more detailed map of expected amplification effects due the local seismostratigraphical configuration has been determined by accounting for relevant uncertainty. Moreover, the impact of these effects on the seismic hazard has been also evaluated by considering the inherent probabilistic character of this estimate.

The approach here considered can be summarized as follows. First, geological, geophysical and geotechnical data relative to the study area have been collected and reanalysed. Since relatively deep seismic impedance contrasts are expected to exist in the area, main attention has been devoted to the reconstruct the seismostratigraphical profile down to depths of the order of hundreds of meters. Second, outcomes of an extensive passive seismic survey (H/V technique) have been used to provide a first zoning of the urban area into microzones area where the local seismostratigraphical configuration is expected to be nearly homogeneous. For each microzone, a representative H/V curve has been inverted to retrieve the local Vs profile by using as a constraint close DH data relative to the shallowest subsoil. These 'master' profiles have been used to constrain the inversion of all H/V measurements available in the respective microzone. Based on borehole data, these profiles have been interpreted in terms of lithostratigraphic units by determining local thickness variations these units and attributing to each of them a range of Vs values. Third, numerical interpolation procedure has been then used to reconstruct a detailed grid map of the seismostratigraphic units in the area. At each node of the grid, a numerical simulation of the expected seismic response has been performed by considering uncertainty affecting the relevant parameterization. Outcomes of this analysis in terms of expected amplification factors (and relevant uncertainty) in different range of periods have been combined with hazard estimates at reference soil conditions to obtain a map of seismic hazard accounting for site effects.

Due to the extensive character of the analysis and the uncertain characterization of the subsoil structure, quantifying and managing relevant uncertainty is of main importance in the assessment of the seismic response to be considered for risk analysis. In our work this aspect has been carefully considered and coherently implemented in the hazard estimates by accounting for the inherent probabilistic character of this kind of estimate.

Outcomes of our study indicate that the choice of the reference seismic bedrock plays a major role in the hazard assessment. This choice cannot be simply demanded to conventional choices. In the case here considered, the definition of the reference seismic bedrock (half space

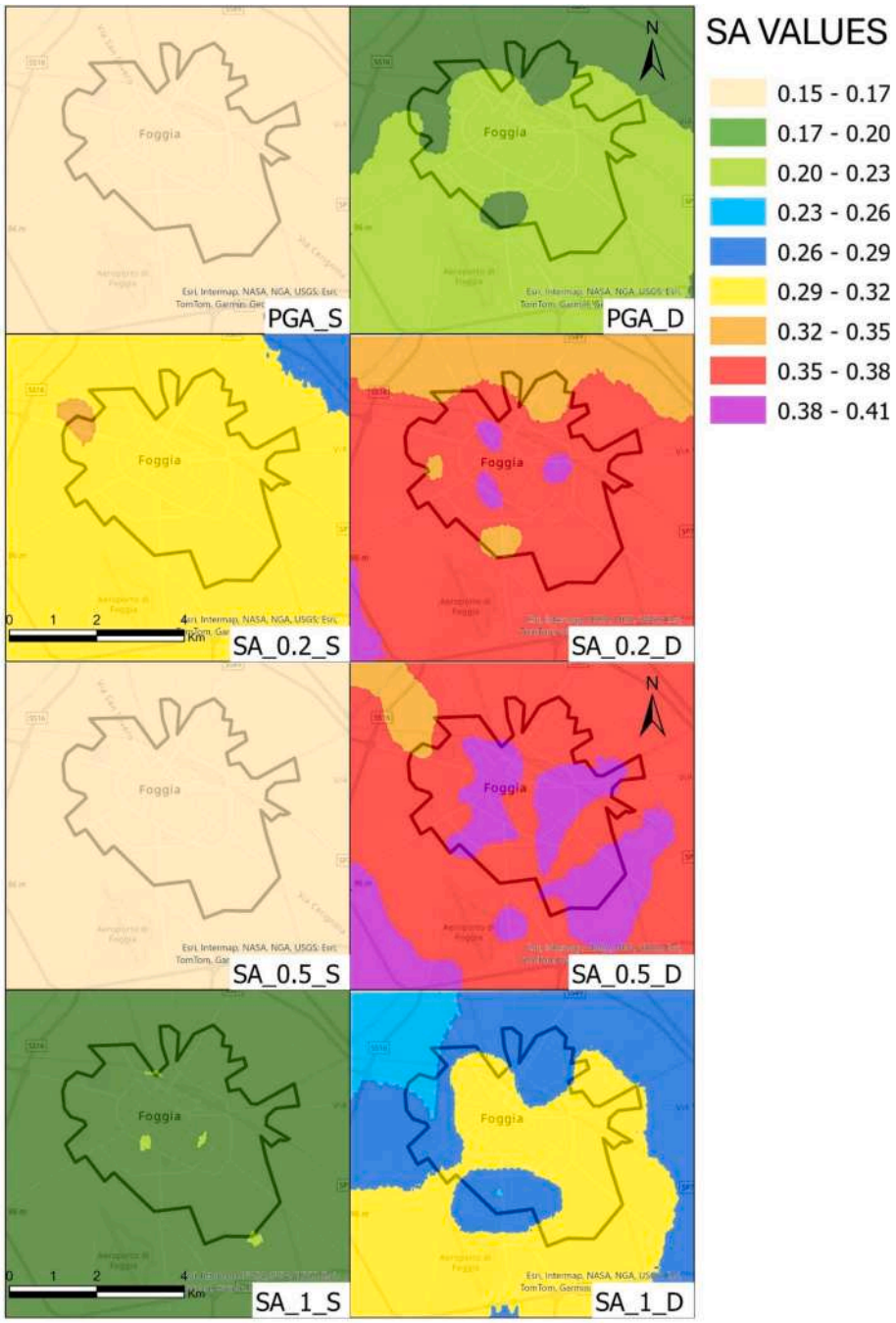

Fig. 10. Spatial distribution of corrected pseudo-acceleration values (SA), expressed in terms of fraction of gravity acceleration (g), for four different spectral periods: 0 s (PGA), 0.2 s, 0.5 s, and 1 s. Each period is shown for both reference seismic bedrock configurations: shallow (S, left column) and deep (D, right column), respectively corresponding to the use of the S-2 and Ls layers in site response simulations. All maps are referenced to the urban area of Foggia. SA values were obtained by applying the obtained amplification factors to the national seismic hazard baseline values corresponding to a 10 % probability of exceedance in 50 years. Colour intervals are consistent across maps and represent increasing levels of ground shaking. See supplementary material for the values obtained at each node of the grid considered for numerical simulations.

with Vs above 800 m/s) can be applied to different interfaces and the choice of the one to be considered significantly affect outcomes. As concerns the case of Foggia, this study demonstrates that the use of a deeper reference seismic bedrock (carbonate layer) leads to higher amplification factors and higher expected seismic effects, particularly for longer periods. These results underscore the importance of carefully defining the reference seismic bedrock boundaries in microzonation studies to ensure a more accurate assessment of local seismic risks. This problem is particularly important and troublesome when the study area is located over a deep sedimentary basin, and the position of the possible reference seismic bedrock can be determined only approximately based on indirect observations. In this regard, results here described may be of help for a critical revision of hazard estimates worldwide, where deep sedimentary basins are present. In particular, the search for eventual strong seismic impedance contrasts at depth, well beyond the typical depth of few tens of meters considered in the common engineering practice, should be encouraged and implemented in local seismic codes. Results obtained in this work also support the joint use of use of numerical simulations and passive seismic methods, such as H/V from ambient vibrations, to constrain Vs profiles at relatively large depths.

This approach appears mandatory when the characterization of local seismic response over wide urban areas located over deep sedimentary basins is of concern and budget limitations do not allow the application of more direct approaches. In these cases, however, uncertainty affecting outcomes must be carefully accounted for and implemented hazard estimates within a coherent probabilistic approach.

Given the extensive character of our analysis, by no way results obtained could be considered as alternative to small scale evaluation of the local seismic response for engineering purposes. The main use of our outcomes is supporting local Authorities for city planning activities devoted to seismic risk reduction at the scale of the whole Municipality. Moreover, they can help to identify most critical situations where more detailed studies are of main importance. Finally, these may supply useful indications about the main constraints to be considered in the detailed seismic response study, such as, in the case of Foggia, the choice of a reference seismic bedrock well below few tens of meters of depth as in most common studies.

Despite the encouraging results obtained, some methodological limitations should be acknowledged. First of all, the whole seismic response analysis assumes that eventual 2D/3D effects play a minor role with respect to vertical heterogeneities. This hypothesis is supported by observing that lateral seismic impedance contrasts are largely lower than the vertical ones. None of the data gathered in the area suggests the presence of significant sharp discontinuities close to the surface (faults, etc.). Another limitation of the analysis here presented concerns the use of the linear equivalent approach for the simulation of the local seismic response. This approximate numerical approach is widely accepted and represents a standard practice in engineering-scale seismic microzonation, especially when studies are constrained by limited data availability or resources, as is the case here. However, one should be aware that, particularly in areas where high amplification and thick clay layers are observed, the linear-equivalent procedure may overestimate the amplification patterns in terms of absolute amplification level and cannot correctly account for resonant frequencies and hysteric soil behaviour (Hosseini Mir Mohammad et al., 2010).

Finally, one must be aware that hazard estimates here proposed only rely on numerical simulations since no direct experimental indication (see, e.g., Primofiore et al., 2020) is available in the area able to support the amplification effects here estimated due to the lack of significant accelerometric registrations representative of reference site conditions at the site of Foggia. It is worth noting however, that relatively high hazard values have been obtained in correspondence of the historical part of the city where main damages were observed during the 1731 earthquake (https://storing.ingv.it/cfti/cfti5/quake.php?01667IT).

CRediT authorship contribution statement

N. Putrino: Writing – review & editing, Writing – original draft, Visualization, Data curation. **G. Cardillo:** Supervision, Investigation, Data curation. **N. Carfagna:** Writing – review & editing, Software, Data curation. **D. Albarello:** Writing – review & editing, Supervision, Conceptualization.

Declaration of competing interest

The authors declare the following financial interests/personal relationships which may be considered as potential competing interests:

Dario Albarello reports administrative support and article publishing charges were provided by University of Siena Department of Physics Earth and Environmental Sciences. If there are other authors, they declare that they have no known competing financial interests or personal relationships that could have appeared to influence the work reported in this paper.

Acknowledgements

Many thanks are due to dr. Albachiara Brindisi for her kind assistance in the application of inversion codes. We are also grateful to the two anonymous referees for their comments and suggestions which allowed us to improve the text.

Appendix A. Supplementary data

Supplementary data to this article can be found online at https://doi.org/10.1016/j.enggeo.2025.108369.

Data availability

Outcomes of the analysis are reported as supplementary material

References

Acunzo, G., Falcone, G., di Lernia, A., Mori, F., Mendicelli, A., Naso, G., Albarello, D., Moscatelli, M., 2024. NC92Soil: a computer code for deterministic and stochastic 1D equivalent linear seismic site response analyses. Comput. Geotech. 165, 105857. https://doi.org/10.1016/j.compgeo.2023.105857.

Albarello, D., Paolucci, E., 2024. Possible measure of soil factors in the Italian seismic code. Bull. Earthq. Eng. 22 (15), 7299–7321.

Albarello, D., Herak, M., Lunedei, E., Paolucci, E., Tanzini, A., 2023. Simulating H/V spectral ratios (H/V) of ambient vibrations: a comparison among numerical models. Geophys. J. Int. 234. https://doi.org/10.1093/gji/ggad109.

Andreotti, G., Famà, A., Lai, C.G., 2018. Hazard-dependent soil factors for site-specific elastic acceleration response spectra of Italian and European seismic building codes. Bull. Earthq. Eng. 16, 5769–5800. https://doi.org/10.1007/s10518-018-0422-9.

Arai, H., Tokimatsu, K., 2004. S-wave velocity profiling by inversion of microtremor H/V spectrum. Bull. Seismol. Soc. Am. 94, 53–63. https://doi.org/10.1785/0120030028.

Boggs Jr., S., 2006. Principles of Sedimentology and Stratigraphy, 4th edition. Pearson Education Inc., Upper Saddle River, p. 662.

Cardillo G., 2021. Microzonazione Sismica della Città di Foggia - Relazione Illustrativa. Regione Puglia, Technical Report, 132 pp.

CEN (European Committee for Standardization), 2005. Part 1: general rules, seismic actions and rules for buildings. In: Eurocode 8: Design of Structures for Earthquake Resistance, EN 1998-1, Brussels.

Cornell, C.A., 1968. Engineering seismic risk analysis. Bull. Seismol. Soc. Am. 58 (5), 1583–1606. https://doi.org/10.1785/BSSA0580051583.

Di Giacomo, D., Gallipoli, M.R., Mucciarelli, M., Parolai, S., Richwalski, S.M., 2005. Analysis and modeling of H/V in the presence of a velocity inversion: the case of Venosa, Italy. Bull. Seismol. Soc. Am. 95 (6), 2364–2372.

Everitt, B.S., Landau, S., Leese, M., 2001. Cluster Analysis, fourth ed. Arnold, London.

Fäh, D., Kind, F., Giardini, D., 2001. A theoretical investigation of average H/V ratios. Geophys. J. Int. 145 (2), 535–549. https://doi.org/10.1046/j.0956-540x.2001.01406.x.

Falcone, G., Boldini, D., Martelli, L., Amorosi, A., 2020. Quantifying local seismic amplification from regional charts and site-specific numerical analyses: a case study. Bull. Earthq. Eng. 18 (1), 77–107.

Falcone, G., Acunzo, G., Mendicelli, A., Mori, F., Naso, G., Peronace, E., Moscatelli, M., 2021. Seismic amplification maps of Italy based on site-specific microzonation dataset and one-dimensional numerical approach. Eng. Geol. 289, 106170.

Foti, S., Parolai, S., Albarello, D., Picozzi, M., 2011. Application of surface-wave methods for seismic site characterization. Surv. Geophys. 32, 777–825. https://doi.org/10.1007/s10712-011-9134-2.

Gaudiosi, I., Romagnoli, G., Albarello, D., Fortunato, C., Imprescia, P., Stigliano, F., Moscatelli, M., 2023. Shear modulus reduction and damping ratios curves joined with engineering geological units in Italy. Sci Data 10 (1), 625. https://doi.org/10.1038/s41597-023-02412-8.

Hosseini Mir Mohammad, S.M., Asadolahi Pajouh, M., Hosseini Mir Mohammad, F., 2010. The limitations of equivalent linear site response analysis considering soil nonlinearity properties. In: International Conferences on Recent Advances in Geotechnical Earthquake Engineering and Soil Dynamics, p. 14. https://scholarsmine.mst.edu/icrageesd/05icrageesd/session03b/14.

ISPRA (Istituto Superiore per la Protezione e la Ricerca Ambientale), 2025. Archivio dei sondaggi. https://www.isprambiente.gov.it/it/attivita/suolo-e-territorio/archivio-dei-sondaggi-ex-lege-464-84.

Joyner, W.B., Warrick, R.E., Fumal, T.E., 1981. The effect of Quaternary alluvium on strong ground motion in the Coyote Lake, California, earthquake of 1979. Bull. Seismol. Soc. Am. 71, 1333–1349. https://doi.org/10.1785/BSSA0710041333.

Kottke, A.R., Rathje, E.M., 2008. Technical Manual for Strata, PEER Report 2008–10. Pacific Earthquake Engineering Research Center, University of California, Berkeley, CA.

Kramer, S.L., 1996. Geotechnical Earthquake Engineering. Prentice Hall, New York.

Lanzo, G., Pagliaroli, A., 2012. Seismic site effects at near-fault strong-motion stations along the Aterno River Valley during the Mw=6.3 2009 L'Aquila earthquake. Soil Dyn. Earthq. Eng. 40, 1–14. ISSN 0267-7261. https://doi.org/10.1016/j.soildyn.2012.04.004.

Lanzo, G., Silvestri, F., Costanzo, A., d'Onofrio, A., Martelli, L., Pagliaroli, A., Simonelli, A., 2011. Site response studies and seismic microzoning in the Middle Aterno valley (L'Aquila, Central Italy). Bull. Earthq. Eng. 9 (5), 1417–1442.

Locati, M., Camassi, R., Rovida, A., Ercolani, E., Bernardini, F., Castelli, V., Caracciolo, C. H., Tertulliani, A., Rossi, A., Azzaro, R., D'Amico, S., Antonucci, A., 2022. Database Macrosismico Italiano (DBMI15), Versione 4.0. Istituto Nazionale di Geofisica e Vulcanologia (INGV). https://doi.org/10.13127/DBMI/DBMI15.4.

McBratney, A.B., Webster, R., 1986. Choosing functions for semi-variograms of soil properties and fitting them to sampling estimates. Eur. J. Soil Sci. 37, 617–639. https://doi.org/10.1111/j.1365-2389.1986.tb00392.x.

McGuire, R.K., 1976. FORTRAN computer program for seismic risk analysis. In: United States Geological Survey Open-File Report No. 76–67. U.S. Geological Survey, Washington DC. https://doi.org/10.3133/ofr7667.

Ministero delle Infrastrutture e dei Trasporti (NTC), 2018. Norme tecniche per le costruzioni. Decreto Ministeriale del 17 gennaio 2018, Supplemento ordinario alla Gazzetta Ufficiale n. 42 del 20 febbraio 2018 (in italian).

Molnar, S., Cassidy, J.F., Castellaro, S., Cornou, C., Crow, H., Hunter, J.A., Matsushima, S., Sanchez-Sesma, F.J., Yong, A., 2018. Application of microtremor horizontal-to-vertical spectral ratio (MH/V) analysis for site characterization: state of the art. Surv. Geophys. 39, 613–631. https://doi.org/10.1007/s10712-018-9464-4.

Mori, F., Gaudiosi, I., Tarquini, E., Bramerini, F., Castenetto, S., Naso, G., Spina, D., 2020. HSM: a synthetic damage-constrained seismic hazard parameter. Bull. Earthq. Eng. 18 (12), 5631–5654.

Moscatelli, M., Albarello, D., Scarascia Mugnozza, G., Dolce, M., 2020. The Italian approach to seismic microzonation. Bull. Earthq. Eng. 18. https://doi.org/10.1007/s10518-020-00856-6.

Nakamura, Y., 1989. A method for dynamic characteristics estimation of the subsurface using microtremor on the ground surface. Q. Rep. RTRI 30, 25–33.

Oliver, M.A., Webster, R., 1990. Kriging: a method of interpolation for geographical information systems. Int. J. Geogr. Inf. Syst. 4 (3), 313–332. https://doi.org/10.1080/02693799008941549.

OPCM 3274, 2003. Ordinanza del Presidente del Consiglio dei Ministri n. 3274 del 20 Marzo 2003. Dipartimento della Protezione Civile. Available at: https://www.protezionecivile.gov.it/.

Pagliaroli, A., Moscatelli, M., Raspa, G., Naso, G., 2014. Seismic microzonation of the central archaeological area of Rome: results and uncertainties. Bull. Earthq. Eng. 12 (3), 1405–1428.

Paolucci, E., Cavuoto, G., Cosentino, G., Coltella, M., Simionato, M., Cavinato, G.P., Albarello, D., 2021. Large-scale seismic characterization of shallow subsoil of Northern Apulia (Southern Italy). Geosciences 2021 (11), 416. https://doi.org/10.3390/geosciences11100416.

Park, C., Miller, R.D., Xia, J., 1999. Multichannel analysis of surface waves (MASW). Geophysics 64 (3), 800–808. https://doi.org/10.1190/1.1444590.

Parolai, S., Picozzi, M., Richwalski, S.M., Milkereit, C., 2005. Joint inversion of phase velocity dispersion and H/V ratio curves from seismic noise recordings using a genetic algorithm, considering higher modes. Geophys. Res. Lett. 320. https://doi.org/10.1029/2004GL021115.

Picozzi, M., Albarello, D., 2007. Combining genetic and linearized algorithms for a two-step joint inversion of Rayleigh wave dispersion and H/V spectral ratio curves. Geophys. J. Int. 169, 189–200.

Picozzi, M., Parolai, S., Richwalski, S.M., 2005. Joint inversion of H/V ratios and dispersion curves from seismic noise: estimating the S-wave velocity of bedrock. Geophys. Res. Lett. 32, 32. https://doi.org/10.1029/2005GL022878.

Pieruccini, P., Fantozzi, P.L., Carfagna, N., Gaudiosi, I., Albarello, D., 2024. Mapping 1D seismic amplification effects in the range of periods of engineering interest based on geological data. Eng. Geol. 341, 107701. https://doi.org/10.1016/j.enggeo.2024.107701.

Primofiore, I., Baron, J., Klin, P., Laurenzano, G., Muraro, C., Capotorti, F., Vessia, G., 2020. 3D numerical modelling for interpreting topographic effects in rocky hills for seismic microzonation: the case study of Arquata del Tronto hamlet. Eng. Geol. 279, 105868.

Puglia, R., Albarello, D., Gorini, A., Luzi, L., Marcucci, S., Pacor, F., 2011. Extensive characterization of Italian accelerometric stations from single station ambient vibration measurements. Bull. Earthq. Eng. 9 (6), 1839–1854. https://doi.org/10.1007/s10518-011-9305-z.

Rafavich, F., Kendall, C.S.C., Todd, T.P., 1984. The relationship between acoustic properties and the petrographic character of carbonate rocks. Geophysics 49, 1622–1636. https://doi.org/10.1190/1.1441570.

Romagnoli, G., Tarquini, E., Porchia, A., Catalano, S., Albarello, D., Moscatelli, M., 2022. Constraints for the Vs profiles from engineering-geological qualitative characterization of shallow subsoil in seismic microzonation studies. Soil Dyn. Earthq. Eng. 161, 107347. https://doi.org/10.1016/j.soildyn.2022.107347.

Santucci de Magistris, F., d'Onofrio, A., Penna, A., Puglia, R., Silvestri, F., 2014. Lessons learned from two case histories of seismic microzonation in Italy. Nat. Hazards 74 (3), 2005–2035.

SM Working Group, 2015. Guidelines for seismic microzonation. In: Conference of Regions and Autonomous Provinces of Italy.

Stucchi, M., Meletti, C., Montaldo, V., Crowley, H., Calvi, G.M., Boschi, E., 2011. Seismic hazard assessment (2003–2009) for the Italian building code. Bull. Seismol. Soc. Am. 101 (4), 1885–1911. https://doi.org/10.1785/012010013.

Vessia, G., Laurenzano, G., Pagliaroli, A., Pilz, M., 2021. Seismic site response estimation for microzonation studies promoting the resilience of urban centers. Eng. Geol. 284, 106031. https://doi.org/10.1016/j.enggeo.2021.106031.